

Final Draft
of the original manuscript:

Lu, X.; Blawert, C.; Mohedano, M.; Scharnagl, N.; Zheludkevich, M.L.;
Kainer, K.U.:

**Influence of electrical parameters on particle uptake during
plasma electrolytic oxidation processing of AM50 Mg alloy**

In: Surface and Coatings Technology (2016) Elsevier

DOI: [10.1016/j.surfcoat.2016.02.006](https://doi.org/10.1016/j.surfcoat.2016.02.006)

Influence of electrical parameters on particle uptake during plasma electrolytic oxidation processing of AM50 Mg alloy

Xiaopeng Lu^{*}, Carsten Blawert, Marta Mohedano, Nico Scharnagl, Mikhail L. Zheludkevich,
Karl Ulrich Kainer

Institute of Materials Research, Helmholtz-Zentrum Geesthacht, Max-Planck-Str. 1, 21502
Geesthacht, Germany

Corresponding author: Phone: +494152871943, Fax: +494152871960,

Email: xiaopeng.lu@hzg.de

Abstract

The influence of electrical parameters on microstructure and composition of coatings by plasma electrolytic oxidation (PEO) with particle addition was investigated. PEO coatings were produced on AM50 magnesium alloy from an alkaline phosphate based electrolyte (1 g/l KOH + 20 g/l Na₃PO₄) with 5 g/l SiO₂ particle (1-5 μm) addition. Besides the most common electrical parameters (voltage and current density), frequency and duty ratio have effect on the uptake of particles during PEO processing. Higher duty ratio and lower frequency allow to incorporate more particles into the PEO coating. The area of the melting pools, as indicated by the size and area of the open pores on the coating surface, can be considered as one important factor to determine the particle uptake during PEO processing.

Keywords

Magnesium; Coatings; Plasma electrolytic oxidation; SiO₂ particle; Electrical parameter

1. Introduction

Plasma electrolytic oxidation (PEO) is a promising surface treatment process derived from conventional anodizing to form ceramic-like coatings on light alloys (Al, Mg and Ti), which are used for corrosion, wear protection and biomedical applications [1-5]. PEO uses aqueous eco-friendly, usually alkaline, electrolytes and the coatings are formed by high voltage, when short-lived discharges occur locally on the coating surface leading to a high pressure and temperature environment [6, 7]. Regarding Mg and its alloys, a two- or three-layer structure is typically observed with a characteristic thin barrier layer laying directly on the metal surface, of a few hundred nanometers thickness, and an outer porous layer which exhibits relatively low corrosion resistance [8, 9]. The properties of the coating mainly depend on the substrate, treatment time, electrical regime (DC, AC and bipolar) and electrolyte, where the electrolyte plays a decisive role due to the incorporation of species from the bath into the oxide film [10, 11].

Introducing particles to the PEO electrolyte, such as clay, ZrO_2 , CeO_2 , Si_3N_4 , Al_2O_3 , SiO_2 , SiC and hydroxyapatite (HA), have been explored as new strategies to seal pores and provide a wider range of compositions for PEO coatings on Mg/Mg alloys [12-20]. Metal oxide particles (e.g. Fe_3O_4 and ZrO_2) can also be incorporated into the coatings by adding related metal salts to the electrolyte [21, 22]. Besides the electrolyte parameters and treated matrix, the process parameters such as applied voltage/current density, frequency and duty cycle have a significant influence on the coating microstructure and properties [23-25], which will also determine the uptake and incorporation of particles during PEO processing. It is expected that the amount of incorporated particles will be in direct relation to the applied voltage and current density, since the dispersed particles in the alkaline electrolyte are negatively charged [26] and will move towards the anode continuously. Therefore, higher voltage and current density will result in a higher number of incorporated particles together with other components from the electrolyte. So far, there are only

a limited number of reports about the effect of frequency and duty ratio on particle addition during PEO processing.

2. Experimental

Specimens of AM50 magnesium alloy with a size of 15 mm × 15 mm × 4 mm were prepared from gravity cast ingot material. The chemical composition of AM50 alloy, as measured with an Arc Spark OES (Spark analyser M9, Spectro Ametek, Germany), is 4.74 wt.% Al, 0.383 wt.% Mn, 0.065 wt.% Zn, 0.063 wt.% Si, 0.002 wt.% Fe, 0.002 wt.% Cu and Mg balance. The specimens were ground using emery papers up to 1200 grit and then air-dried prior to PEO treatment.

The PEO process was carried out by using a pulsed DC power source with different frequencies and pulse ratios, as shown in Table 1. Pulse-on and pulse-off time were varied to study the effect on the particle uptake. The specimens and a stainless steel tube were used as the anode and cathode, respectively. 5 g/l of SiO₂ particles in the range of 1-5 μm were added into a phosphate based electrolyte (1 g/l KOH and 20 g/l Na₃PO₄). A stirrer and bubbling generator were used to facilitate the uniform distribution of the particles in the electrolyte. All the PEO treatments were performed at a constant voltage of 450 V for 10 min and the average current density provided by the DC power supply was limited to 300 mA/cm². The temperature of the electrolytes was kept at 10 ± 2 °C by a water cooling system.

A scanning electron microscope (TESCAN Vega3 SB) combined with an energy dispersive spectrometer (EDS) system from eumeX (ixrfsystems) was used to examine the surface morphology, composition and microstructure of the PEO coatings. An acceleration voltage of 15 kV was applied for SEM and EDS investigations. According to the EDS analysis, the Si content of the same specimen between different positions was nearly the same (< 5 %). The phase crystal

structure analysis was done with a Bruker X-ray diffractometer using Cu K α radiation. Image analysis software analySIS pro 5.0 was used to measure the number and size of the pores on coating surface.

3. Results and discussion

3.1. Microstructure

The effect of frequency and duty ratio on the surface morphology of the resulting coatings is shown in Fig. 1. Regardless of the duty ratio, the surface of the coatings at 50 Hz condition contains relatively large pores in comparison to coatings produced by use of higher frequencies (250 and 500 Hz). In other words, the specimens coated at higher frequencies result in much higher pore density, constituted from smaller and uniformly distributed pores. As for the influence of duty ratio on coating surface, it is obvious that the size of the pores becomes larger with the increase of the duty ratio, resulting in a more porous PEO coating. It is also worth to note that the pores of the coating surface produced from 500 Hz and 10 % duty ratio are smaller than those of the other coatings. After quantitative analysis of the open pores (0.22 mm² surface area), the number and the total area of the pores on coating surface are given in Fig. 2. With the increase of frequency, the number of the pores on coating surface is increasing. For low duty ratio (10 %), the pore number increases from 90 ± 4 (50 Hz) to 242 ± 18 (250 Hz) and 378 ± 24 (500 Hz). A similar trend can also be observed when using high duty ratio. In the case of total area, it is decreasing with higher frequency and lower duty ratio. For instance, the total area of the pores of the coating obtained from the same duty ratio (10 %) decrease from 17696 ± 1200 μm^2 (50 Hz) to 14508 ± 850 μm^2 (250 Hz) and 13889 ± 610 μm^2 (500 Hz). In other words, lower frequency and higher duty ratio enable PEO coating to have less number of pores but with larger area.

According to Fig. 3, the thickness of the PEO coating is influenced significantly by the applied frequency and duty ratio. Higher duty ratio and lower frequency produce thicker PEO coatings. For example, the coating thickness decreases from $84 \pm 7 \mu\text{m}$ (50 Hz) to $45 \pm 5 \mu\text{m}$ (250 Hz) and $35 \pm 4 \mu\text{m}$ (500 Hz) at low duty ratio. Therefore, coating produced at 50 Hz with 30 % duty ratio has the thickest layer, which means the growth rate is higher than for other conditions. Moreover, cross section of the coatings produced by different frequencies with 10 % duty ratio was prepared by embedding the specimens into resin, as can be seen in Fig. 4. These observations corroborate the eddy current probe thickness measurements since there is not too much error between the different techniques. It was reported that lower frequency could provide higher growth rate for PEO coating [27], which is consistent with the observations of the current work. The coatings are composed of two layers, an outer porous layer and an inner barrier layer. A pore band between the outer layer and inner layer is clearly observed, which is normally stated for PEO coatings produced from phosphate based electrolyte [28, 29].

Fig. 5 demonstrates the distribution of SiO_2 particles on the surface and cross section of the coating produced from treatment with 50 Hz and 10% duty ratio. Plenty of particles can be found on the coating surface (Fig. 5a), indicating that the uptake of the particles is via the coating/electrolyte interface. In addition, a small region lack of particles can be observed at the lower right corner of the selected image. It can be inferred that the last discharge has not melted this region since it is too far away from the discharge channel. As shown in Fig. 5b, the particles are distributed randomly across the whole layer. It is worth to note that the outer layer of the coating has been detached from the inner layer at the location of the pore band. Based on the mapping results, there is nearly no Si signal in the same region at the inner part of the coating in comparison to P and O, suggesting that the ending position for particles penetration through a coating is the pore band.

3.2. Phase and chemical composition

The X-ray diffraction patterns of the coatings are depicted in Fig. 6a. It can be seen that all the coatings are composed of amorphous phase in the 2θ range of $20\text{--}35^\circ$, possibly containing phosphorus, except the small amount of MgO. The appearance of magnesium peaks in all conditions is due to the penetration of the X-ray through the whole layer and reaching the substrate. SiO_2 peaks are also visible, indicating that the micro-sized particles are inertly incorporated into PEO coating. This is consistent with our previous investigations [29]. In order to study the influence of electrical parameters on particle uptake, EDS analysis was performed on the surface of all the coated specimens and the Si content is presented in Fig. 6b. It is found that the Si content is decreasing with the increasing frequency, and higher duty ratio enables PEO coating with more particles, which might be attributed to the relatively longer pulse-on time per pulse. For instance, less amount of Si (3.8 at. %) was detected for coating produced at higher frequency (500 Hz with 10% duty ratio) compared with the coating obtained from lower frequency, e.g., 5.6 at. % (250 Hz) and 6.9 at. % (50 Hz). It is worthwhile to note that the tendency of the incorporated particles is similar to the trend of the total area of the pores and coating thickness, which are most likely to be controlled by the applied frequency and duty ratio. Thus changing the pulse-on or pulse-off time is necessary to be further investigated to identify the role of electrical parameters in the uptake of particles during PEO processing.

3.3. Influence of pulse-on and pulse-off time on particle uptake

Coating produced at 250 Hz with 10 % duty ratio was used as the standard coating for this study. To identify the effect of pulse-on and pulse-off time on particle uptake during PEO process, either the pulse-on or the pulse-off time of a single pulse will be changed. First, the pulse-off time was changed from 3.6 ms to 1.8 ms and 7.2 ms. The resultant coating microstructure is shown in Fig. 7. After reducing the pulse-off time, the coating thickness decreases and becomes

nonuniform, as the thickness of the layer reduces from $41 \pm 7 \mu\text{m}$ to $20 \pm 11 \mu\text{m}$. However, the coating thickness ($40 \pm 4 \mu\text{m}$) is not influenced greatly when increasing the pulse-off time from 3.6 ms to 7.2 ms. As for the particle content, there is no significant effect of pulse-off time on uptake of particle into PEO coating. The Si content is nearly the same for all the three coatings, 6.3 at. % (0.4 ms + 1.8 ms), 6.0 at. % (0.4 ms + 3.6 ms) and 6.1 at. % (0.4 ms + 7.2 ms), respectively.

In case of pulse-on time, it seems to markedly affect the uptake of the external particles into PEO coatings. Fig. 8 shows the surface and cross section of the coatings obtained from different pulse-on time, namely, 0.2 ms + 3.6 ms and 0.8 ms + 3.6 ms in comparison to the standard coating (0.4 ms + 3.6 ms). It is apparent that longer pulse-on time could produce more porous coating, since the size of the open pores on the coating surface are becoming uneven and larger to some extent. Meanwhile, increase the pulse-on time of a single pulse leads to formation of a thicker layer, as the coating thickness increases from $28 \pm 9 \mu\text{m}$ (0.2 ms) to $41 \pm 7 \mu\text{m}$ (0.4 ms) and $49 \pm 6 \mu\text{m}$ (0.8 ms). With regard to the Si content, the particle concentration increases linearly from 5 at. % to 6 at. % and 7.2 at. %, indicating that pulse-on time plays an important role in the particle uptake during PEO treatment.

3.4. Role of pores on coating surface in particle uptake

There is no doubt that the applied electrical parameters determine the formation of the PEO coating. Like other anions in the electrolyte, the negatively charged particles will move towards the anode with the aid of applied electric field. The main electrochemical reactions occurring at the coating/electrolyte interface during PEO processing is the dissolution of the Mg and subsequent combination with anions (OH^- and PO_4^{3-}) from the electrolyte. As the discharges are unavoidable for PEO process, the coating material will be melted by the high temperature and ejected outwards. As a consequence, melting pools appear on the coating surface accompanying

with the discharges, leading to adhesion of some anions in the electrolyte/coating interface, including the particles. Large-sized pores on the coating surface are indications of strong discharges, which can absorb large number of anions and result in thicker layer. The mixture of the original material with the new absorbed anions will flow back after the discharge extinguishes. It is unlikely for particles which are larger than the discharge channel to flow back during solidification process, which means that large-sized particles will remain on the coating surface instead of entering into the inward coating, while some small-sized particles might pass through the open pores on the coating surface reaching the internal layer. Therefore, uptake of particles into PEO coating is mainly via sticking on the melting pools that are generated by the discharges during PEO processing. In short, the surface area of the melting pool, as indicated by the size and total area of the pores on the coating surface which are mainly dependent on the applied electrical parameters, can be considered as an important factor to determine the particle uptake during PEO processing.

4. Conclusions

- 1) The area of the melting pool, as indicated by the pores, on the coating surface is responsible for the particle uptake. Particles can directly enter into the coating via open pores, but mainly by sticking on the coating surface.
- 2) Lower frequency and higher duty ratio produce PEO coatings with large-area and large-sized pores, leading to uptake of more particles.
- 3) Pulse-on time of per pulse is more important than pulse-off time for particle uptake during PEO processing.

Acknowledgements

The technical support of Mr. Volker Heitmann and Mr. Ulrich Burmester during the course of this work is gratefully acknowledged. X. Lu thanks China Scholarship Council for the award of fellowship and funding. M. Mohedano is grateful to the Alexander von Humboldt Foundation, Germany, for the award of AvH research fellowship and financial assistance.

References

- [1] A.L. Yerokhin, A. Shatrov, V. Samsonov, P. Shashkov, A. Pilkington, A. Leyland, A. Matthews, Oxide ceramic coatings on aluminium alloys produced by a pulsed bipolar plasma electrolytic oxidation process, *Surf. Coat. Technol.*, 199 (2005) 150-157.
- [2] S. Yagi, K. Kuwabara, Y. Fukuta, K. Kubota, E. Matsubara, Formation of self-repairing anodized film on ACM522 magnesium alloy by plasma electrolytic oxidation, *Corros. Sci.*, 73 (2013) 188-195.
- [3] M. Mu, J. Liang, X. Zhou, Q. Xiao, One-step preparation of TiO₂/MoS₂ composite coating on Ti6Al4V alloy by plasma electrolytic oxidation and its tribological properties, *Surf. Coat. Technol.*, 214 (2013) 124-130.
- [4] G. Wu, J.M. Ibrahim, P.K. Chu, Surface design of biodegradable magnesium alloys — A review, *Surf. Coat. Technol.*, 233 (2013) 2-12.
- [5] Y. Song, K. Dong, D. Shan, E.H. Han, Study of the formation process of titanium oxides containing micro arc oxidation film on Mg alloys, *Appl. Surf. Sci.*, 314 (2014) 888-895.
- [6] R.O. Hussein, X. Nie, D.O. Northwood, An investigation of ceramic coating growth mechanisms in plasma electrolytic oxidation (PEO) processing, *Electrochim. Acta*, 112 (2013) 111-119.
- [7] R.O. Hussein, D.O. Northwood, X. Nie, Coating growth behavior during the plasma electrolytic oxidation process, *J. Vac. Sci. Technol. A*, 28 (2010) 766-773.
- [8] J.E. Gray, B. Luan, Protective coatings on magnesium and its alloys - a critical review, *J. Alloy. Compound.*, 336 (2002) 88-113.
- [9] R. Arrabal, E. Matykina, P. Skeldon, G.E. Thompson, Coating formation by plasma electrolytic oxidation on ZC71/SiC/12p-T6 magnesium metal matrix composite, *Appl. Surf. Sci.*, 255 (2009) 5071-5078.
- [10] A.L. Yerokhin, X. Nie, A. Leyland, A. Matthews, Characterisation of oxide films produced by plasma electrolytic oxidation of a Ti-6Al-4V alloy, *Surf. Coat. Technol.*, 130 (2000) 195-206.
- [11] R. Arrabal, E. Matykina, T. Hashimoto, P. Skeldon, G.E. Thompson, Characterization of AC PEO coatings on magnesium alloys, *Surf. Coat. Technol.*, 203 (2009) 2207-2220.
- [12] R. Arrabal, E. Matykina, F. Viejo, P. Skeldon, G.E. Thompson, M.C. Merino, AC plasma electrolytic oxidation of magnesium with zirconia nanoparticles, *Appl. Surf. Sci.*, 254 (2008) 6937-6942.

- [13] K.M. Lee, K.R. Shin, S. Namgung, B. Yoo, D.H. Shin, Electrochemical response of ZrO₂-incorporated oxide layer on AZ91 Mg alloy processed by plasma electrolytic oxidation, *Surf. Coat. Technol.*, 205 (2011) 3779-3784.
- [14] T.S. Lim, H.S. Ryu, S.-H. Hong, Electrochemical corrosion properties of CeO₂-containing coatings on AZ31 magnesium alloys prepared by plasma electrolytic oxidation, *Corros. Sci.*, 62 (2012) 104-111.
- [15] X. Li, B.L. Luan, Discovery of Al₂O₃ particles incorporation mechanism in plasma electrolytic oxidation of AM60B magnesium alloy, *Mater. Lett.*, 86 (2012) 88-91.
- [16] D. Sreekanth, N. Rameshbabu, Development and characterization of MgO/hydroxyapatite composite coating on AZ31 magnesium alloy by plasma electrolytic oxidation coupled with electrophoretic deposition, *Mater. Lett.*, 68 (2012) 439-442.
- [17] X. Lu, C. Blawert, N. Scharnagl, K.U. Kainer, Influence of incorporating Si₃N₄ particles into the oxide layer produced by plasma electrolytic oxidation on AM50 Mg alloy on coating morphology and corrosion properties, *J. Magnesium Alloy.*, 1 (2013) 267-274.
- [18] M. Mohedano, C. Blawert, M.L. Zheludkevich, Silicate-based Plasma Electrolytic Oxidation (PEO) coatings with incorporated CeO₂ particles on AM50 magnesium alloy, *Mater. Des.*, 86 (2015) 735-744.
- [19] X. Lu, C. Blawert, M.L. Zheludkevich, K.U. Kainer, Insights into plasma electrolytic oxidation treatment with particle addition, *Corros. Sci.*, 101 (2015) 201-207.
- [20] L. Yu, J. Cao, Y. Cheng, An improvement of the wear and corrosion resistances of AZ31 magnesium alloy by plasma electrolytic oxidation in a silicate-hexametaphosphate electrolyte with the suspension of SiC nanoparticles, *Surf. Coat. Technol.*, 276 (2015) 266-278.
- [21] S. Lu, W. Qin, X. Wu, X. Wang, G. Zhao, Effect of Fe³⁺ ions on the thermal and optical properties of the ceramic coating grown in-situ on AZ31 Mg Alloy, *Mater. Chem. Phys.*, 135 (2012) 58-62.
- [22] H. Li, S. Lu, X. Wu, W. Qin, Influence of Zr⁴⁺ ions on solar absorbance and emissivity of coatings formed on AZ31 Mg alloy by plasma electrolytic oxidation, *Surf. Coat. Technol.*, 269 (2015) 220-227.
- [23] X.H. Wu, P.B. Su, Z.H. Jiang, S. Meng, Influences of Current Density on Tribological Characteristics of Ceramic Coatings on ZK60 Mg Alloy by Plasma Electrolytic Oxidation, *Acs Appl. Mater. Interfaces*, 2 (2010) 808-812.
- [24] R.O. Hussein, P. Zhang, X. Nie, Y. Xia, D.O. Northwood, The effect of current mode and discharge type on the corrosion resistance of plasma electrolytic oxidation (PEO) coated magnesium alloy AJ62, *Surf. Coat. Technol.*, 206 (2011) 1990-1997.
- [25] R.O. Hussein, D.O. Northwood, X. Nie, The effect of processing parameters and substrate composition on the corrosion resistance of plasma electrolytic oxidation (PEO) coated magnesium alloys, *Surf. Coat. Technol.*, 237 (2013) 357-368.
- [26] K.M. Lee, B.U. Lee, S.I. Yoon, E.S. Lee, B. Yoo, D.H. Shin, Evaluation of plasma temperature during plasma oxidation processing of AZ91 Mg alloy through analysis of the melting behavior of incorporated particles, *Electrochim. Acta*, 67 (2012) 6-11.

[27] P. Bala Srinivasan, J. Liang, R.G. Balajee, C. Blawert, M. Störmer, W. Dietzel, Effect of pulse frequency on the microstructure, phase composition and corrosion performance of a phosphate-based plasma electrolytic oxidation coated AM50 magnesium alloy, *Appl. Surf. Sci.*, 256 (2010) 3928-3935.

[28] X. Lu, S.P. Sah, N. Scharnagl, M. Störmer, M. Starykevich, M. Mohedano, C. Blawert, M.L. Zheludkevich, K.U. Kainer, Degradation behavior of PEO coating on AM50 magnesium alloy produced from electrolytes with clay particle addition, *Surf. Coat. Technol.*, 269 (2015) 155-169.

[29] X. Lu, C. Blawert, Y. Huang, H. Ovri, M.L. Zheludkevich, K.U. Kainer, Plasma electrolytic oxidation coatings on Mg alloy with addition of SiO₂ particles, *Electrochim. Acta*, 187 (2016) 20-33.

Figure captions

Fig. 1: Surface morphology of the coatings produced from different frequencies and duty ratios (a) 50 Hz and 10 %, (b) 250 Hz and 10 %, (c) 500 Hz and 10 %, (d) 50 Hz and 30 %, (e) 250 Hz and 30 %, (f) 500 Hz and 30 %.

Fig. 2: Number (a) and total area (b) of the pores on coating surface at a magnification of $500 \times$ (0.22 mm^2 surface area).

Fig. 3: Thickness of the PEO coatings.

Fig. 4: Cross section of the PEO coatings produced from different frequencies and duty ratios (a) 50 Hz and 10 %, (b) 250 Hz and 10 %, (c) 500 Hz and 10 %, (d) 50 Hz and 30 %, (e) 250 Hz and 30 %, (f) 500 Hz and 30 %.

Fig. 5: EDS maps of the PEO coatings obtained from 50 Hz and 10 % (a) surface and (b) cross section.

Fig. 6: XRD patterns (a) and Si content (b) of the PEO coatings.

Fig. 7: Surface and cross section morphology of the coatings produced from different pulse-off time (a-d) 0.4 ms +1.8 ms, (e, f) 0.4 ms +7.2 ms.

Fig. 8: Surface and cross section morphology of the coatings produced from different pulse-on time (a, b) 0.2 ms +3.6 ms, (c, d) 0.8 ms +3.6 ms.

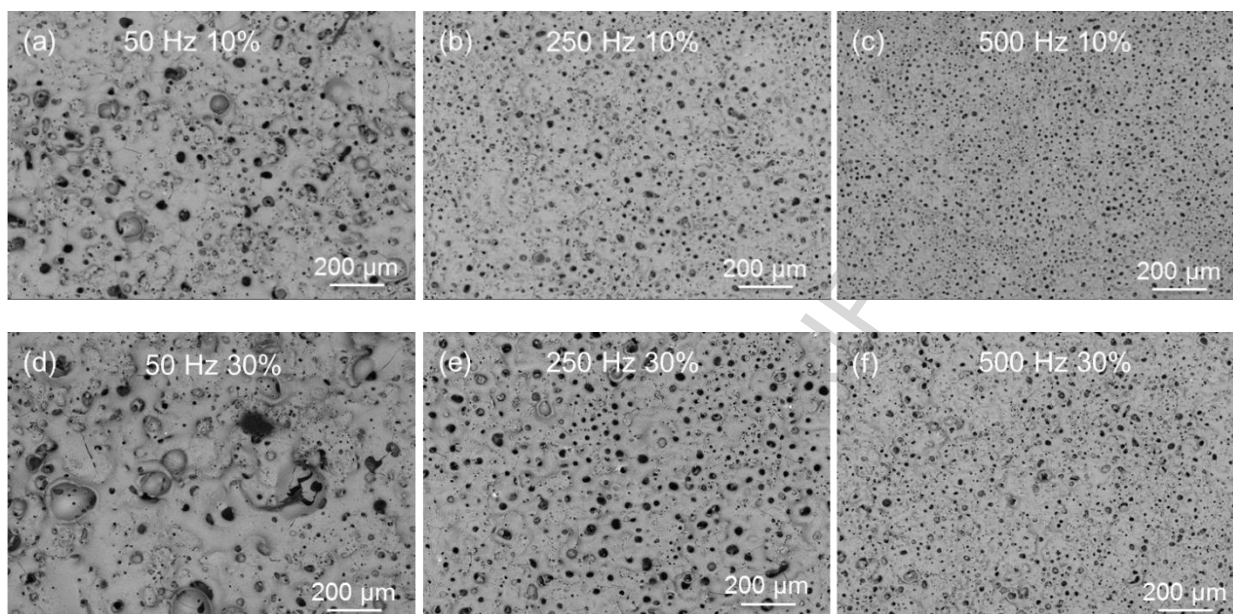


Figure 1

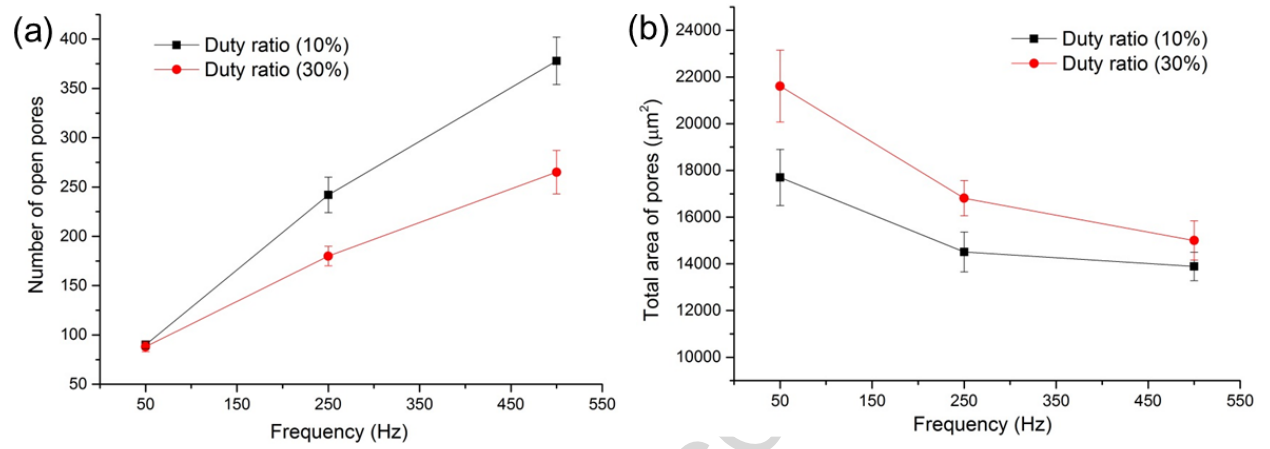


Figure 2

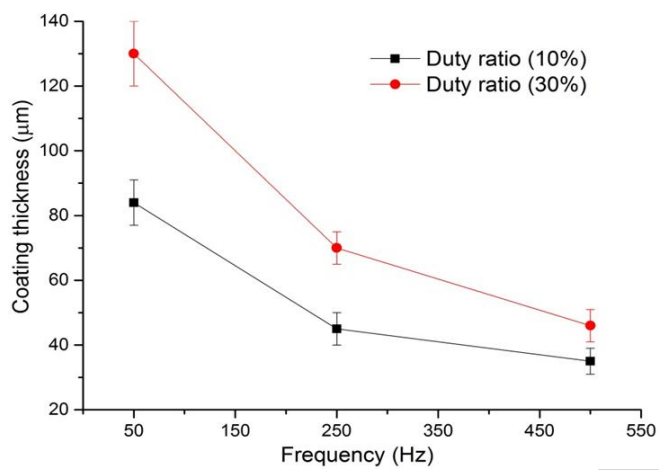


Figure 3

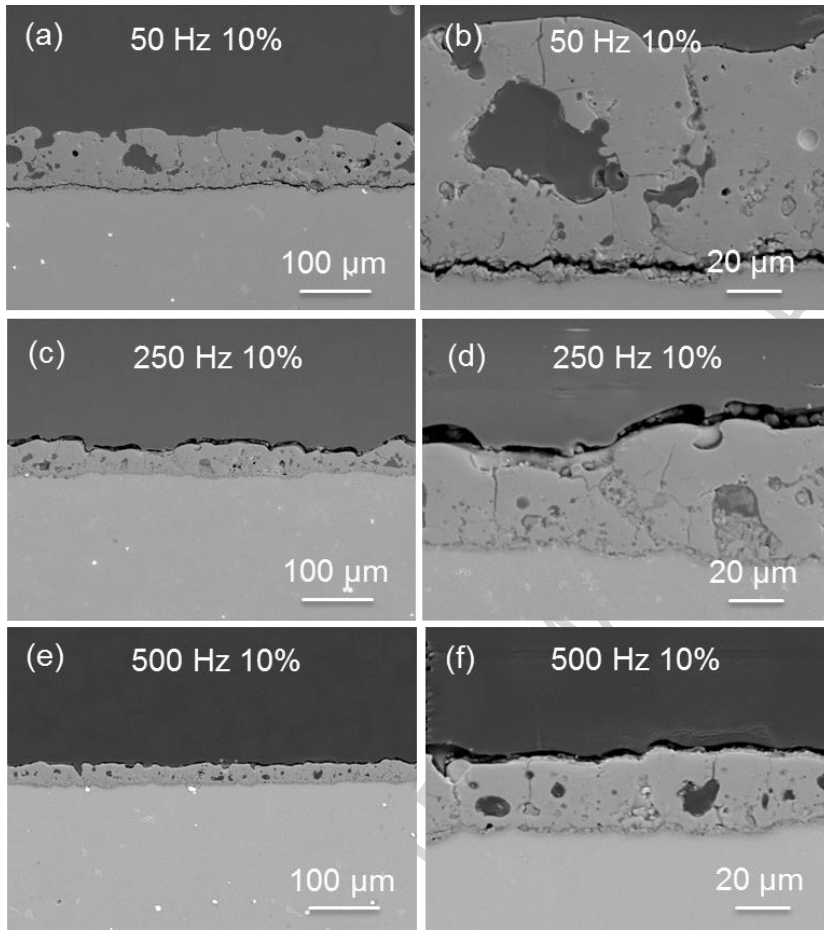


Figure 4

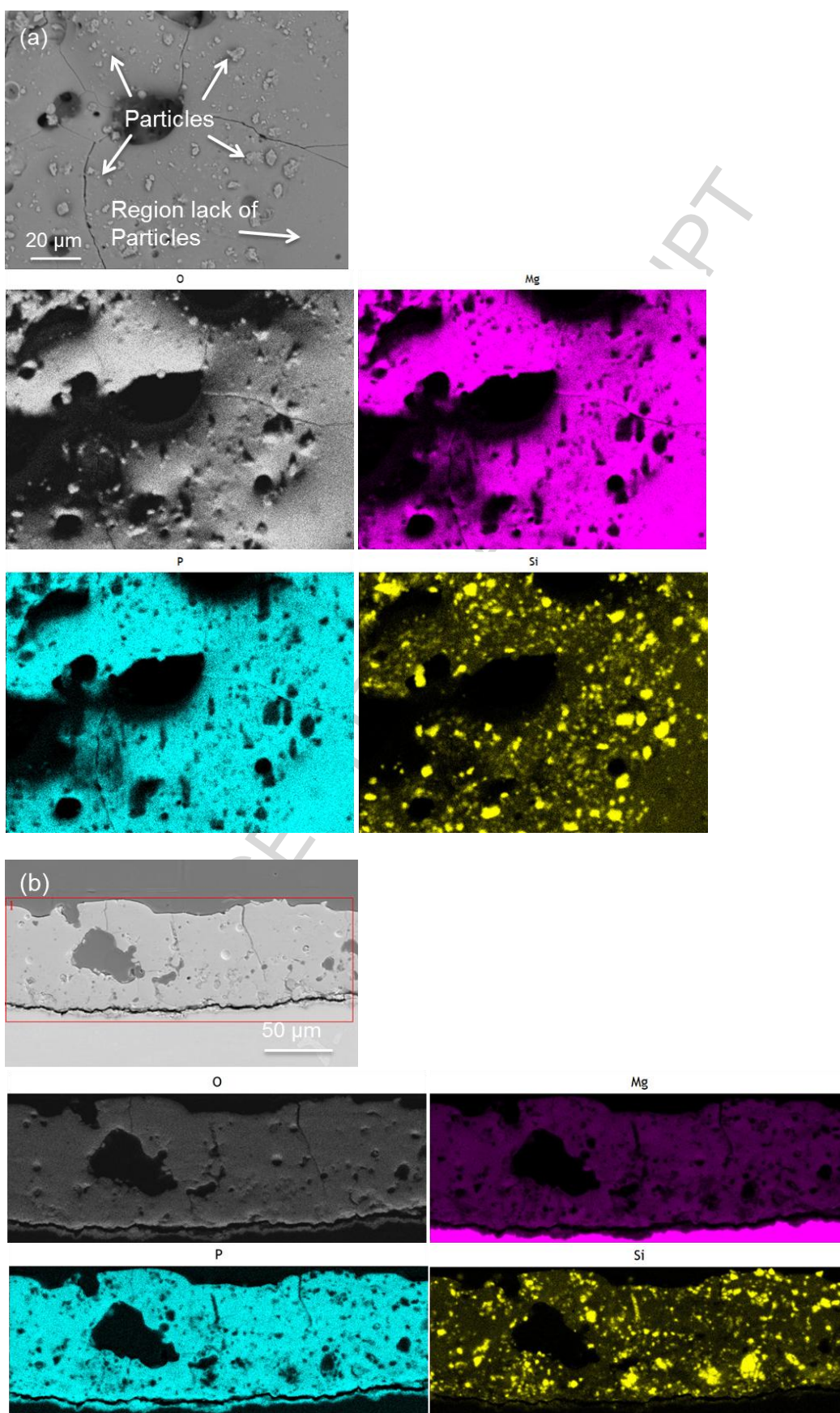


Figure 5

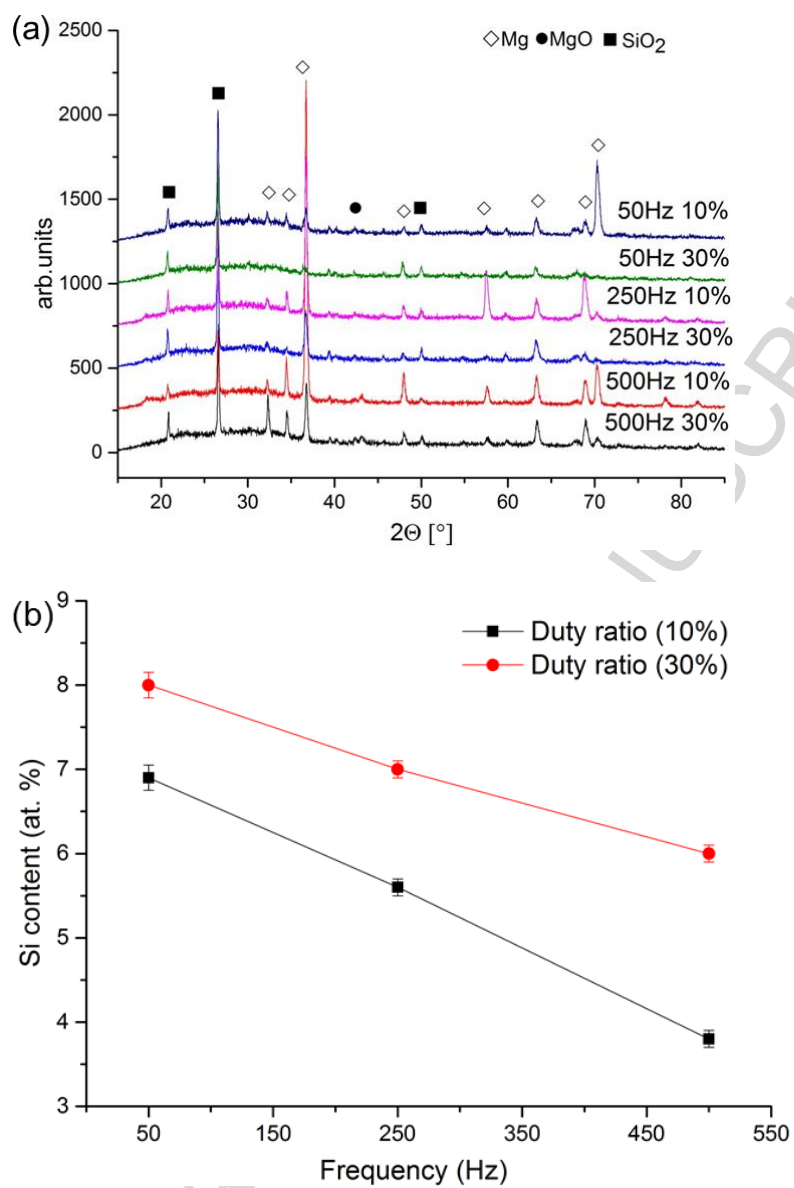


Figure 6

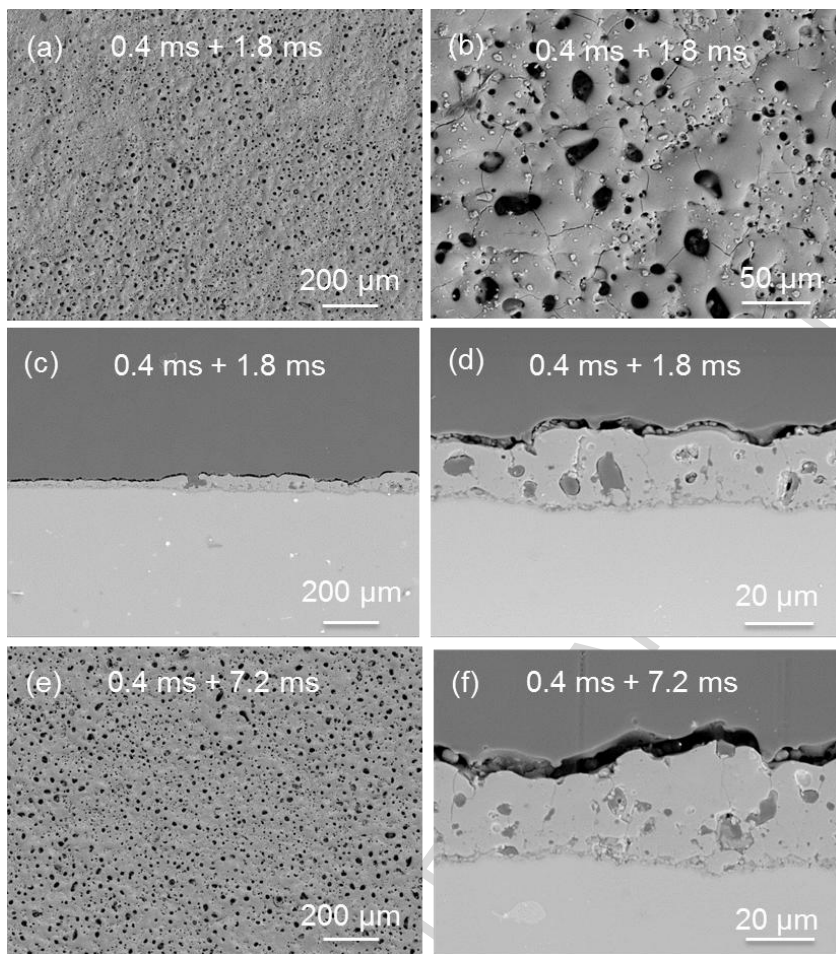


Figure 7

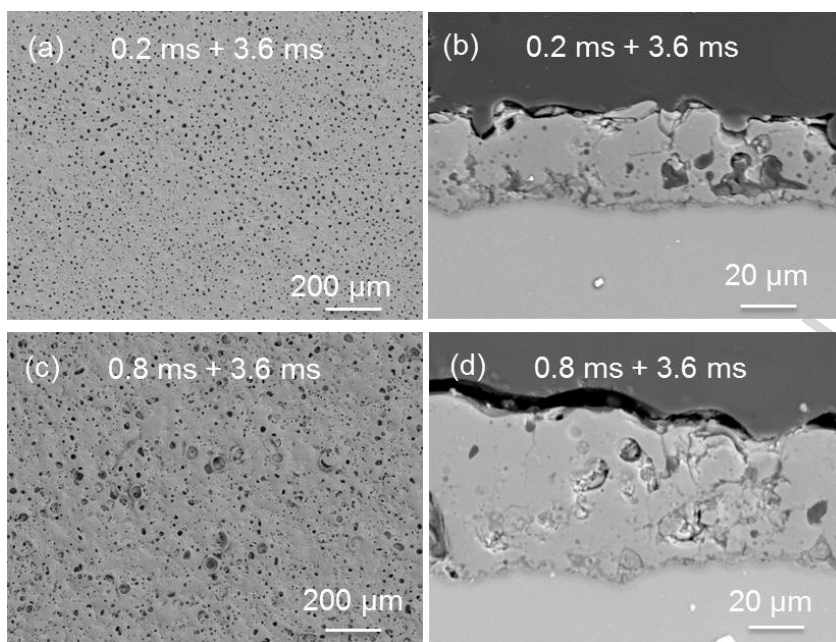


Figure 8

Table 1. Electrical parameters used for PEO treatment.

Frequency and duty ratio	Pulse-on and pulse-off time (ms)
50 Hz and 10 %	2 + 18
250 Hz and 10 %	0.4 + 3.6
500 Hz and 10 %	0.2 + 1.8
50 Hz and 30 %	6 + 14
250 Hz and 30 %	1.2 + 2.8
500 Hz and 30 %	0.6 + 1.4

Highlights

- The area of the melting pool on coating surface is responsible for particle uptake.
- Low frequency and high duty ratio produce high porosity for PEO coatings.
- Pulse-on time is more important than pulse-off time for particle uptake.